8th International IFAC Symposium on
Dynamics and Control of Process Systems
Preprints Vol.2, June 6-8, 2007, Cancún, Mexico

# MODELING AND OPTIMIZATION OF THE THERMAL BEHAVIOR OF A SILICON STEEL DECARBURIZATION PROCESS

**Cláudia M. Silva[1], Milton M. Silva[2], Márcio Ziviani[3]**

*1- Chemtech - A Siemens Company - Rua da Quitanda, 50/21º andar, Centro, CEP 20011-030 - Rio de Janeiro, RJ*
*2- Acesita S.A. - Praça 1º de Maio, 9, Centro, CEP 35180-018 - Timóteo, MG*
*3- Departamento de Engenharia Mecânica - UFMG - Av. Antônio Carlos, 6627, CEP 31270-901 - Belo Horizonte, MG*

Abstract: Optimal operation conditions of a silicon steel strip production have been investigated by means of a theoretical study on a tunnel-shaped thermal equipment. A mathematical model has been developed to describe the thermal process occurring in a continuous load moving through sections of electrical radiant heaters and forced coolers. The proposed methodology evaluates both radiative exchange and convective transfer. The simulated results provide the workload temperature distribution profile in any equipment position. Model validation was obtained by confronting the simulated and experimental results obtained by ACESITA S.A. Optimal conveying speed and heating sector temperatures were determined by using a particle swarm optimization algorithm.


Keywords: Magnetic properties, heat exchangers, heat flows, mathematical modeling, optimization problems, heuristic searches, finite difference method, temperature profiles.

## 1. INTRODUCTION

Silicon electrical steels are higher grade steels that present noble electromagnetic properties. Such steels have their properties optimized by means of a rigorously controlled carbon oxidation process, which provides them with high permeability and low core loss. Grain-oriented electrical steels have their magnetic flux density developed in the coil rolling direction and a glass-like surface that provides insulation. They are used in stationary applications, like in transformers, but also in electrical equipment cores, for high-efficiency electric motors and generators.

High amount of silicon inhibits eddy currents and narrows the hysteresis loop of the material, thus lowering the core losses and increasing electrical resistance. The carbon content, conversely, increases eddy currents and hysteresis losses while decreasing the steel permeability. It also increases susceptibility of the steel to magnetic aging, resulting in an increase in power loss over time. Therefore, the carbon level of silicon steels should be kept as lower as 0.005%.

Carbon removal from the steel is achieved through reaction with dissolved gases by a process commonly known as decarburization. The material is submitted to a heat treatment performed under a moistened nitrogen atmosphere containing small amounts of hydrogen. Annealing the steel in such decarburizing atmosphere causes carbon oxidation on the steel surface by the oxidizing gases. The consequent reduction in the amount of soluble carbon and in the volume fraction of carbides reduces magnetic losses and increases resistance to magnetic aging.

The heat treatment usually involves the steel being heated into a temperature in the austenite phase field, which ranges from 800 to 1200 $^{o}$C, depending on the chemical composition of the processed material.

During the heat treatment, a vast range of microstructures are produced in the steel surface, which generates specific mechanical properties. The quality of the final product is strongly dependent on the treatment intrinsic conditions as well as on the temperature, as such conditions simultaneously influence the chemical reactions.

Due to the highly sophisticated technology involved, several studies on the production of this type of steel have been conducted in the last few years. Special attention has been given to the modeling and simulation of industrial thermal equipments.

Federov *et al.* (1998) presented a methodology to simulate heating process in a continuous load furnace. The thermal model was used to define the design parameters of an industrial furnace, such as the optimal temperature of the heat source required to reach a prescribed temperature distribution on the surface load. Carvalho (2003) developed a mathematical model to simulate and control the annealing process of steel strips in a continuous industrial natural gas fired furnace. The thermal energy balance involves the gas combustion heat generation, the absorbed energy, the heat losses due to smoke flow rate, the energy required to increase the internal temperature and heat losses through openings. Kang *et al.* (2004) proposed a mathematical model to describe the thermal behavior of fused or forget metal pieces in a continuous furnace. The model calculates the temperature profile as a function of the load relative position inside the furnace. Gorni *et al.* (2000) evaluated the performances of the Finite Difference Method and the Finite Element Method in solving the thermal profile of a slab reheating furnace. They simulated the temperature behavior over three selected slab depths in the pre-heating, heating and soaking sections. The performances of the methods were compared by means of Pearson's correlation coefficient, **r**, and the estimate standard deviation. These authors claimed that the Finite Element Method had a better global performance, predicting the slab discharging temperature with a greater degree of accuracy. The Finite Difference Method, however, presented the best performance results for the simulation case carried out with the depth value closer to the slab surface.

This contribution aims to investigate the behavior of the temperature profiles in the silicon steel strip production at ACESITA S.A, in order to identify the best operation conditions for the industrial electrical furnace in use. For this reason, the radiative heat exchange and convective heat transfer that occurs during the electrical steel production have been precisely described through mathematical models, to ensure the prediction of the optimal process conditions. A mathematical model has been proposed to describe the thermal profile of the steel strip during the decarburization process (Silva, 2006) based on the available process parameters. The model simulates the heating and cooling phases, when the material is submitted to variations of temperature, conveying speed and atmosphere composition.

## 2. EQUIPMENT DESCRIPTION

The decarburization thermal reactor comprises two main sections for material treatment – the heating and cooling sections, and three peripheral equipments – gas mixture station, power systems and moisture system. The equipment schematic representation is illustrated in Figure 1.

The equipment performs complete thermal cycles producing superficial and structural transformations in the steel strip, based on chemical reactions rigorously controlled. The heating process is carried out by a system of electrical resistors distributed along the furnace ceiling, floor and lateral walls. The heating and soaking sections comprise nine control zones of distinct lengths and specific installed power. The temperature is controlled by monitoring selected locations of the furnace and comparing the pre-defined temperature set points with the measured and registered ones. Following the heating phase, the steel strip is submitted to a controlled cooling phase that is performed in three sections – static cooling, water-cooled heat exchange and gas jet cooling.

The bulk atmosphere consists of a mixture of hydrogen, nitrogen and water vapor, maintained at a rigorously controlled concentration to accomplish the required specific chemical reactions. The moisturizing level of the gas mixture is indirectly controlled by the atmosphere dew point.

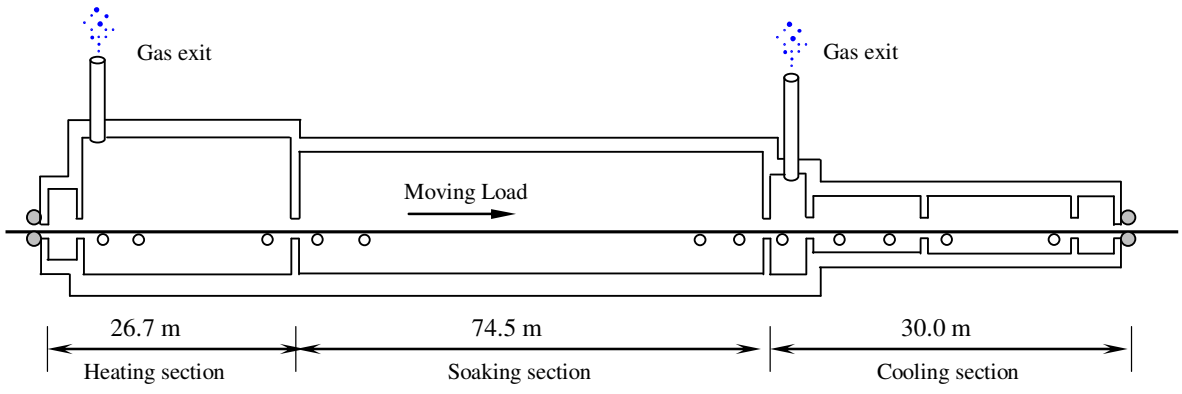


Fig. 1 - Schematic representation of the thermal equipment

## 3. MATHEMATICAL MODEL

A mathematical model has been developed to describe the heating and cooling process that occurs in a continuous load at constant conveying speed through sections of electrical radiant heaters and of forced coolers of an industrial furnace. In order to simplify the numerical solution problem, all zones presenting similar thermal characteristics were grouped together. The resulting reactor model consists of seven sectors.

### *3.1 Energy Balance Law*

The energy balance equations for the specific case of a moving steel strip in a thermal equipment, whose internal parameters vary as a function of the position, are represented by the energy conservation law:

$$\frac{D}{Dt}\left(\rho c_p T\right) = div\left(k \nabla T\right) + S \tag{1}$$

where $T$ is the load temperature, $S$ is the volumetric rate of the internal energy source and $D/Dt$ is the substantive derivative. Assuming that the material is homogenous and isotropic, equation (1) can be rewritten in the Cartesian coordinate system as:

$$\rho c_p\left(\frac{\partial T}{\partial t} + u\frac{\partial T}{\partial x} + v\frac{\partial T}{\partial y} + w\frac{\partial T}{\partial z}\right) = \frac{\partial}{\partial x}\left(k\frac{\partial T}{\partial x}\right) + \frac{\partial}{\partial y}\left(k\frac{\partial T}{\partial y}\right) + \frac{\partial}{\partial z}\left(k\frac{\partial T}{\partial z}\right) + S \tag{2}$$

When processing a sequence of coils with similar characteristics, stead state is assumed, and the derivative of the temperature over the time is null ($\partial T/\partial t = 0$). As velocities $v$ and $w$ in the directions $y$ and $z$ are also null, equation (2) becomes:

$$\rho c_p\left(u\frac{\partial T}{\partial x}\right) = \frac{\partial}{\partial x}\left(k\frac{\partial T}{\partial x}\right) + \frac{\partial}{\partial y}\left(k\frac{\partial T}{\partial y}\right) + \frac{\partial}{\partial z}\left(k\frac{\partial T}{\partial z}\right) + S \tag{3}$$

In spite of no internal energy is generated, the source term is kept on the equation, as it represents the combined radiative and convective heat flow that is incident on the horizontal surface of the steel strip:

$$\rho c_p\left(u\frac{\partial T}{\partial x}\right) = \frac{\partial}{\partial x}\left(k\frac{\partial T}{\partial x}\right) + \frac{\partial}{\partial y}\left(k\frac{\partial T}{\partial y}\right) + \frac{\partial}{\partial z}\left(k\frac{\partial T}{\partial z}\right) + \dot{q}_c + \dot{q}_r \tag{4}$$

where $\dot{q}_c$ is the convection heat flow and $\dot{q}_r$ is the radiation heat flow. The source term varies as a function of the characteristics of each thermal sector.

The effect of the diffusion heat transfer is quite small, as a result of the reduced thickness of the strip, which is around 0.27 mm. The diffusion contribution is also considered insignificant when compared to the radiation and convection processes:

$$\dot{q}_c + \dot{q}_r >> \frac{\partial}{\partial x}\left(k\frac{\partial T}{\partial x}\right) + \frac{\partial}{\partial y}\left(k\frac{\partial T}{\partial y}\right) + \frac{\partial}{\partial z}\left(k\frac{\partial T}{\partial z}\right) = q_k\big|_x + q_k\big|_y + q_k\big|_z \tag{5}$$

Therefore, the diffusion term can be disregarded:

$$\rho c_p\left(u\frac{\partial T}{\partial x}\right) = \dot{q}_c + \dot{q}_r \tag{6}$$

Boundary conditions of first specie, in $x$ direction, are considered for the problem:

$$\text{for } x = 0 \quad \Rightarrow \quad T = T_{bulk} \tag{7}$$

### *3.2 The Convective Source Term*

The convective heat transfer process is determined by the correlations between the horizontal surface and a parallel counter current stream. The convective coefficient is calculated by Newton's cooling law, considering the atmosphere conditions in each sector:

$$q_c = h_c A\left(T_s - T_\infty\right) \tag{8}$$

where $h_c$ is the convective heat transfer coefficient, which varies as a function of the thermal sector characteristics. The convective heat exchange between the gas and the steel strip is calculated by the correlation for a parallel stream and a flat surface:

$$Nu_x \equiv \frac{h_x x}{k} = 0.332\left(\mathrm{Re}_x\right)^{1/2}\left(\mathrm{Pr}\right)^{1/3} \tag{9}$$

where $Nu_x$ is the local Nusselt number, $\mathrm{Re}_x$ is Reynolds number and Pr is Prandle number.

The gas jet cooling sector is modeled as colliding jets. The convective heat exchange between the gas and the steel strip is calculated by the following correlations (Incropera and De Witt, 2003):

$$\frac{\overline{Nu}}{\mathrm{Pr}^{0.42}} = K\left(A_r, \frac{H}{D}\right) G\left(A_r, \frac{H}{D}\right) F_2\left(\mathrm{Re}\right) \tag{10}$$

where

$$K = \left[1 + \left(\frac{H/D}{0.6/A_r^{1/2}}\right)^6\right]^{-0.05} \tag{11}$$

$$G = 2A_r^{1/2}\frac{1 - 2.2A_r^{1/2}}{1 + 0.2\left(H/D - 6\right)A_r^{1/2}} \tag{12}$$

$$F_2 = 0.5\,\mathrm{Re}^{2/3} \tag{13}$$

### *3.3 The Radiative Source Term*

The radiative heat exchange is described by the radiative heat transfer law:

$$q_r = \sigma\varepsilon A\left(T_1^4 - T_2^4\right) \tag{14}$$

where $\sigma$ is the Stefan-Boltzmann constant ($5.67e^{-8}$ $W/m^2K^4$) and $\varepsilon$ is the gray-body emissivity of the object whose absolute temperature is $T_1$. The linearized form of the equation (14) is:

$$q_r = h_r A\left(T_1 - T_2\right) \tag{15}$$

where $h_r$ is the radiative heat exchange rate. Stefan-Boltzmann law states that the emissive power from a black body, $E_B$, is directly proportional to the forth power of its absolute temperature, and the emitted power for a non-black body:

$$E_B = \sigma \varepsilon T^4 \tag{16}$$

The radiative heat exchange rate is estimated by considering an enclosure formed by the steel strip surface, the heated and non-heated furnace walls and the hypothetical surfaces (front and back void frontiers and horizontal void surface between the strip and the furnace walls). The heated walls represent the heat source. The non-heated walls are considered isolated and gray surfaces and behave similarly to a diffuse, opaque and isothermal surface. The front and back surfaces of the enclosure and the two void surfaces between the strip and the walls are considered fictitious planar surfaces with the internal atmosphere characteristics. Additional effects on the radiative heat transfer rate, regarded to the gaseous atmosphere, are also considered.

The equivalent thermal circuit for the radiative heat exchanges inside the enclosure is presented in Figure 2. In this figure, $E_B$ is the emissive power, $J$ is the combination of radiation reflected and emitted from a surface and $R$ is the heat transfer resistance. The subscript *SS* stands for steel strip, *F* means frontier, *W* is the furnace wall, *HW* is the heated wall and *HS* the hypothetical surface. The concept of radiation configuration factor, defined as the fraction of diffusely radiated energy leaving a surface A that is incident on the nonoverlapping surfaces B that covers the enclosure, was used. The basic relationships of the configuration factors proposed by Howell (2005) for parallel and perpendicular planes were adopted.

### *3.4 The Numerical Solution*

As the problem cannot be solved analytically, the Finite Difference Method with implicit formulation was used to integrate equation (6) through the moving load direction. The trajectory of a small segment of the steel strip is followed through the furnace sections.

During the integration progress, the segment faces different physical conditions, specific of each furnace section. Thus, the integration of equation (6) has to take into account different boundary conditions, depending on the location of the segment in its trajectory along the furnace.

For the problem integration, the initial condition considers the steel strip at the room temperature. The temperature at the previous position is used as boundary condition to determine the current one. At each integration step, the temperature is iteratively calculated until the convergence, achieved under a tolerance error of $10^{-3}$. The radiative heat exchange, the convective heat transfer, the gaseous mixture properties and steel strip properties are also updated at each integration step.

## 4. MODEL VALIDATION

The mathematical model was developed based on the design and operation parameters of the tunnel-shaped thermal metallurgical equipment at ACESITA S.A. Historical data of the temperature measurements performed on the heating and soaking section during the period of 2002 to 2005 were used to validate the proposed model. Table 1 presents statistic parameters of the steel strip temperature measured in crucial locations for the process control. Figure 3 compares the profiles of the simulated results along the furnace to the measured ones, in order to evaluate the performance of the proposed model.

Table 1 – Historical data of steel strip temperatures measured in heating section (2002 to 2005)

| Zone | Mean (ºC) | Standard deviation |
|---|---|---|
| 3 | 745.3 | 13.3 |
| 4 | 802.2 | 11.1 |
| 5 | 826.8 | 6.5 |
| 6 | 831.4 | 7.6 |
| 7 | 832.6 | 7.8 |
| 8 | 835.2 | 8.6 |
| 9 | 833.2 | 5.1 |

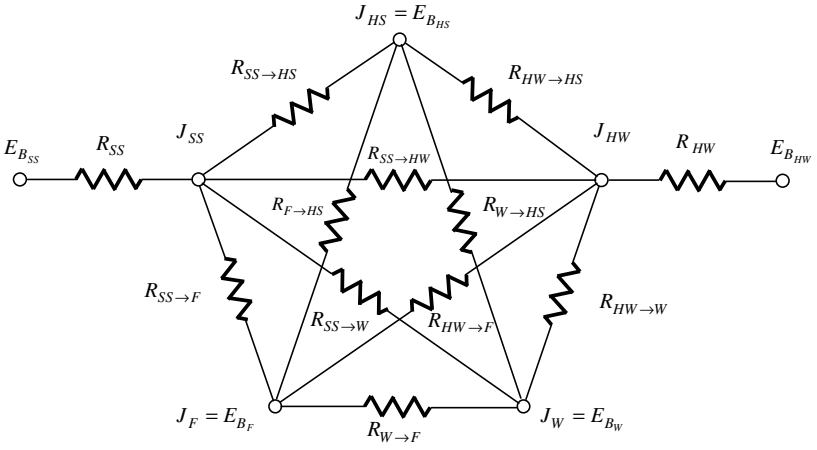


Fig. 2 - The equivalent thermal circuit for the radiative heat exchanges

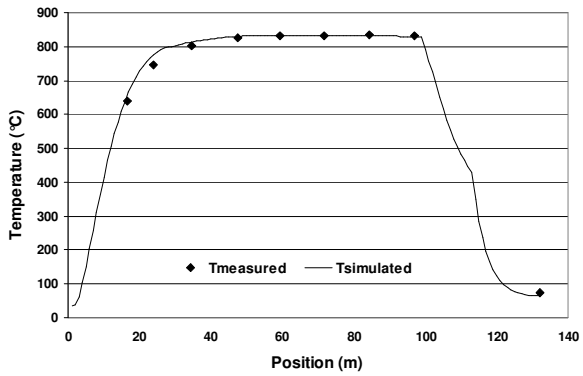


Fig. 3 - Measured and simulated temperature profiles

It can be observed that the proposed methodology provides a good approximation to the experimental results. The deviations listed in Table 2 corroborate this achievement, as the highest discrepancy between the results (around 12%) was obtained in a region where historical measurement data are not available.

Table 2 – Deviations of the simulated temperatures from the measured ones

| Zone | Simulated temperature (°C) | Deviation (°C) | Deviation (%) |
|---|---|---|---|
| 2 | 652.4 | 14.37 | 2.25 |
| 3 | 773.9 | 28.57 | 3.83 |
| 4 | 813.6 | 11.36 | 1.42 |
| 5 | 830.0 | 3.22 | 0.39 |
| 6 | 832.5 | 1.10 | 0.13 |
| 7 | 832.9 | 0.27 | 0.03 |
| 8 | 832.8 | -2.40 | -0.29 |
| 9 | 829.6 | -3.61 | -0.43 |
| exit | 66.0 | -8.68 | -11.62 |

Furthermore, the results obtained along the soaking section, which is considered of major significance to the production quality, presented a maximum deviation of 1.42%.

## 5. OPTIMIZATION PROBLEM

The validated model was used to predict optimal operation conditions for the furnace. An evolutionary algorithm is adopted to solve the optimization problem, due to the ability of such methods to deal with complex nonlinear search spaces.

### *5.1 Particle Swarm Optimization*

Particle Swarm Optimization (PSO) is a stochastic optimization technique developed by Kennedy and Eberhart (1995), based on the social behavior of a swarm. The system is initialized with a population of random solutions in a hyperspace, $R^n$, and searches for optima by updating generations. The potential solutions have their position and velocity adjusted for the search progress based on the memory of their own best position and knowledge of the swarm's best position. The movement of the particles towards the optimum is governed by:

$$\mathbf{v}_i(t+1) = w\mathbf{v}_i(t) + c_1 r_1\left(\mathbf{P}_i(t) - \mathbf{x}_i(t)\right) + c_2 r_2\left(\mathbf{P}_g(t) - \mathbf{x}_i(t)\right) \quad (17)$$

$$\mathbf{x}_i(t+1) = \mathbf{x}_i(t) + \mathbf{v}_i(t+1) \quad (18)$$

where $w$ is an inertial coefficient that balances global and local search, $c_1$ and $c_2$ are constants that say how much the particle's best and the global best influence its movement. $\boldsymbol{P}_i$ is the best position vector of particle $i$, $\boldsymbol{P}_g$ is the best position vector of all particles, $\boldsymbol{x}_i$(t) is the current position vector of particle $i$ and $\boldsymbol{v}_i$(t) is the current velocity of particle $i$. The method comprises a simple concept that can be easily implemented and is computationally inexpensive in terms of both memory requirements and speed. Early studies have shown the efficiency of this method in performing several kinds of problems (Kennedy and Eberhart, 1995).

### *5.2 Problem formulation*

An optimization problem is proposed to increase the steel strip production rate at ACESITA S.A, taking into account the strict temperature specifications required to guarantee the production quality. The aim is to find new set point values of the temperature in each section, which would still provide the steel strip with the required temperature profile when increasing the conveying speed. The objective function consists of a term that accounts for the increase in the plant throughput and a series of terms that penalize deviation in temperature from the desired values at various points along the process. The manipulated variables include the conveying speed, $v$, and set points of the heating temperature, $Th$, the soaking temperature, $Ts$, and the static cooling temperature, $Tsc$:

$$fobj(v, Th, Ts, Tsc) = k_1.v + k_2\sum_{i=1}^{3}\text{abs}(Th_i - Th_m) + k_3\sum_{i=1}^{6}\text{abs}(Ts_i - Ts_m) \quad (19)$$

subject to $0.5 \le v \le 1.5$ m/s, $1000 \le Th \le 1400$ K, $1000 \le Ts \le 1400$ K, $400 \le Tsc \le 1000$ K

where $k_i$ are weight factors and the subscript $m$ stands for measure values. The optimization parameters used are $w$ varying from 0.9 to 0.5, $c_1$ = 1.5 and $c_2$ = 1.5, a population of 10 particles and 200 iterations.

## 6. RESULTS

The optimal conditions obtained are: conveying speed of 0.925 m/s, heating temperature of 1156.3 K, soaking temperature of 1154.2 K and static cooling temperature of 622.0 K. Figure 4 illustrates the deviation of the measured results from the simulated ones, obtained under two conditions: the existent industrial operation parameters and the optimal ones. It can be observed that the operation under the optimal parameters presents very small deviations.

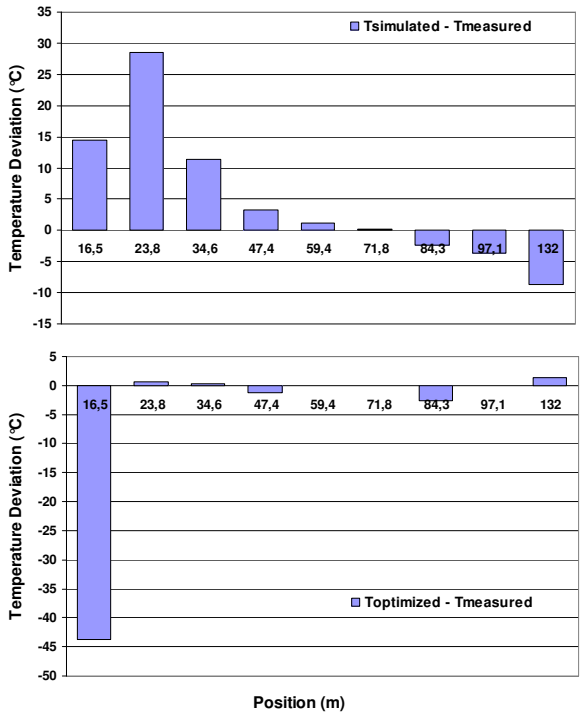


Fig. 4 - Deviations of the simulated and optimized temperatures from the measured ones

Table 3 presents the numerical values for the deviations. In soaking section, the maximum discrepancy from the measured temperatures to the ones simulated under the optimal conditions is 0.31%. Among all the measurements, the greatest difference is around 7%, in a region where the temperature varies drastically and no historical data are available. These results are rather superior to the ones obtained in the previous simulation.

The optimal conditions also provide an increase of 26% in the electrical steel production. The required increase on the reactor internal temperatures, however, is of only 2% in the heating and soaking sections, while in the cooling section a reduction of 17% is allowed. Due to the increase of the production, a reduction of 46 kWh/ton is obtained in the monthly consumption, which represents an annual budget of 2,145,632 kWh and a profit of US$ 142,250.00.

Table 3 – Deviations of the optimized temperatures from the measured ones

| Zone | Optimized temperature (°C) | Deviation (°C) | Deviation (%) |
|---|---|---|---|
| 2 | 594.2 | -43.77 | -6.86 |
| 3 | 746.0 | 0.68 | 0.09 |
| 4 | 802.6 | 0.37 | 0.05 |
| 5 | 825.6 | -1.18 | -0.14 |
| 6 | 831.4 | -0.01 | -0.001 |
| 7 | 832.5 | -0.10 | -0.01 |
| 8 | 832.6 | -2.62 | -0.31 |
| 9 | 833.2 | -0.001 | 0.00 |
| exit | 76.0 | 1.34 | 1.79 |

## 7. CONCLUSION

A detailed mathematical model has been proposed to simulate the temperature profile during the silicon steel strip production at ACESITA S.A. The model describes the radiative and convective heat transfers that occur in a continuous load moving in the tunnel-shaped thermal equipment. A Finite Difference Method with implicit formulation was used to solve the problem. During the integration progress, the segment faces different physical conditions, specific of each furnace section. The model was validated with historical data of the production process.

A Particle Swarm Optimization algorithm was employed to identify the best operational conditions for this furnace. The optimization problem aimed to increase the production rate following the strict temperature specifications required by the chemical reactions. Optimal values for the temperature set point at each section have been determined in order to guarantee the required temperature profiles. The manipulated variables include the conveying speed and the heating, soaking and static cooling temperatures. The optimal conditions obtained provided an increase of 26% in the industrial production, with an increase of only 2% in the energy consumption of the heating and soaking sections, and a decrease of 17% in the cooling section.

## 8. REFERENCES


Carvalho, S. R. (2003). *Desenvolvimento de um Modelo Matemático e Computacional de um Forno de Recozimento.* MSc. Thesis, UFU, Uberlândia.

Fedorov, A. G., K. H. Lee, and R. Viskanta (1998). Inverse Optimal Design of the Radiant Heating in Materials Processing and Manufacturing. *Journal of Materials Engineering and Performance*, Vol. 7 (6), pp. 719-726.

Gorni, A. A., V. B. Formica and O. Bogdan (2000). Comparação entre Abordagens para o Modelamento Matemático do Perfil Térmico de Placas Durante seu Reaquecimento. *Revista Escola de Minas*, Vol. 53, n.3, pp. 203-209.

Howell, J. R. (2005). *A Catalog of Radiation Heat Transfer Configuration Factors. In: Thermal Radiation Heat Transfer*, 4th edition.

Incropera, F. P. and D. P. De Witt (2003). *Fundamentals of Heat and Mass Transfer.* LTC, 5th edition.

Kang, J., T. Huang and R. Purushothaman (2004). Modeling and Simulation of Heat Transfer in Loaded Continuous Heat Treatment Furnace. *Transactions of Materials and Heat Treatment, Proc. 14 th IFHTSE Congress*, Vol. 25, n 5.

Kennedy, J. and R. Eberhart (1995). Particle Swarm Optimization. *Proc. 4th IEEE Int. Conf. on Neural Networks* IEEE, Piscataway, NJ, Vol. 4 pp.1942-1948.

Silva, M. M. (2006). *Modelagem Matemática do Comportamento Térmico do Processo de Descarbonetação de Tiras de Aços Siliciosos.* MSc Thesis, UFMG, Belo Horizonte.